Overlapping DDFV Schwarz algorithms on non-matching grids

Martin J. Gander and Laurence Halpern and Florence Hubert and Stella Krell

1 Introduction

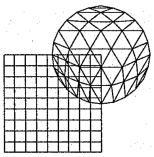

Ever since the publication of the first book on domain decomposition methods by Smith, Bjørstad, and Gropp [8], where non-matching grids were used for overlapping Schwarz methods (see on the right), and the methods worked very well, a theoretical understanding of their convergence remained open. We are interested in a better understanding of such Schwarz methods for Discrete Duality Finite Volume (DDFV) discretizations for anisotropic diffusion,

$$\mathcal{L}(u) := -\mathrm{div}(A\nabla u) = f \text{ in } \Omega, \quad u = 0 \text{ on } \partial\Omega, \quad A(x,y) := \begin{pmatrix} A_{xx} & A_{xy} \\ A_{xy} & A_{yy} \end{pmatrix}, \quad (1)$$

where Ω is an open bounded domain of $\mathbb{R}^2$, and A is a uniformly symmetric positive definite matrix. DDFV optimized Schwarz methods have been developed for (1) in [5, 4], because these techniques are especially well suited for anisotropic diffusion [6, 3, 1]. We study here for the first time a new overlapping DDFV Schwarz algorithm with classical Dirichlet transmission conditions that can handle non-matching grids, due to carefully chosen additional unknowns in the DDFV scheme. We prove convergence of the DDFV

Martin J. Gander
Section de Mathématiques, Université de Genève, e-mail: martin.gander@unige.ch

Laurence Halpern
LAGA, Université Sorbonne Paris-Nord, 93430 Villetaneuse, e-mail: halpern@math.univ-paris13.fr

Florence Hubert
Aix-Marseille Université, CNRS, Centrale Marseille, I2M UMR 7373, 39 rue F. Joliot Curie, 13453 Marseille, Cedex 13, FRANCE, e-mail: florence.hubert@univ-amu.fr

Stella Krell
Université Côte d'Azur, Inria, CNRS, LJAD, France, e-mail: stella.krell@univ-cotedazur.fr

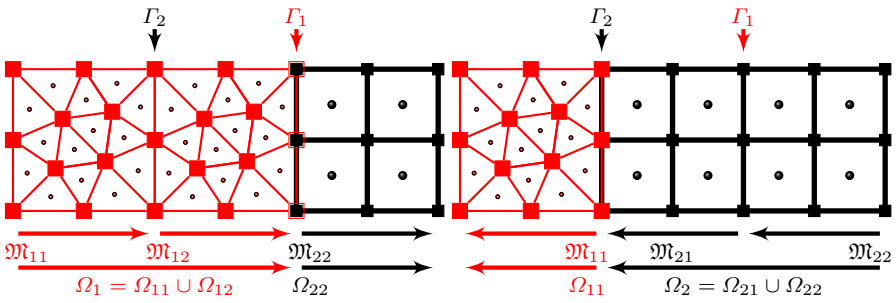

Fig. 1: Primal non-matching meshes associated to the decomposition $\Omega = \Omega_1 \cup \Omega_2$. Left: primal mesh $\mathfrak{M}_1 = \mathfrak{M}_{11} \cup \mathfrak{M}_{12}$ for Ω_1 in red. Right: primal mesh $\mathfrak{M}_2 = \mathfrak{M}_{21} \cup \mathfrak{M}_{22}$ for Ω_2 in black. Both meshes $\mathfrak{M}_j$ are completed to the entire domain to investigate the limit of the method.

Schwarz algorithm in the case of matching grids, and show numerically that for some non-matching grids convergence is still achieved to monodomain DDFV solutions. Finally, under mesh refinement, the Schwarz limit always converges to the underlying continuous monodomain solution.

2 Overlapping DDFV Schwarz algorithm

The continuous parallel Schwarz method for (1) and two subdomains Ω_1 and Ω_2, $\bar{\Omega} = \bar{\Omega}_1 \cup \bar{\Omega}_2$ reads

$$-\mathrm{div}(A\nabla u_j^{l+1}) = f \text{ in } \Omega_j,\ u_j^{l+1} = 0 \text{ on } \partial\Omega_{j,\mathrm{D}},\ u_j^{l+1} = u_i^l \text{ on } \Gamma_j,\ j = 1, 2, \quad (2)$$

where $i = j + 1 \mod 2$ and $\partial\Omega_j = \partial\Omega_{j,\mathrm{D}} \cup \Gamma_j$ with $\Gamma_j \cap \partial\Omega = \emptyset$. Each subdomain $\bar{\Omega}_j$ can be partitioned into $\bar{\Omega}_{jj} \cup \bar{\Omega}_{ji}$ with $\Omega_{ji} = \Omega_{ij} = \Omega_j \cap \Omega_i$. We now introduce the technical description of DDFV, see [1] for more details.
The meshes. Consider for $j = 1, 2$ a DDFV mesh $\mathcal{T}_j = (\mathfrak{M}_j, \mathfrak{M}_j^*, \partial\mathfrak{M}_j, \partial\mathfrak{M}_j^*)$ of the domain Ω_j defined as follows: the primal mesh $\mathfrak{M}_j = \mathfrak{M}_{jj} \cup \mathfrak{M}_{ji}$ is a set of disjoint open polygonal control volumes $\mathrm{K} \subset \Omega_j$ such that $\cup\overline{\mathrm{K}} = \overline{\Omega_j}$. Here $\mathfrak{M}_{jj}$ (resp. $\mathfrak{M}_{ji}$) stands for the control volumes in Ω_{jj} (resp. in Ω_{ji}). In particular, this implies that no primal control volume of $\mathfrak{M}_j$ is crossed by Γ_i. Note also that in general the meshes in the overlap need not be the same, $\mathfrak{M}_{ji} \neq \mathfrak{M}_{ij}$, as shown in Fig. 1. We call the special case when $\mathfrak{M}_{ji} = \mathfrak{M}_{ij}$ the conforming case, and otherwise the non-conforming case. We denote by $\partial\mathfrak{M}_j$ (resp. $\partial\mathfrak{M}_{j,\mathrm{D}}$, $\partial\mathfrak{M}_{\Gamma_j}$) the set of edges of the control volumes in $\mathfrak{M}_j$ included in $\partial\Omega_j$ (resp. $\partial\Omega_{j,\mathrm{D}}$, Γ_j) with $\partial\mathfrak{M}_j = \partial\mathfrak{M}_{j,\mathrm{D}} \cup \partial\mathfrak{M}_{\Gamma_j}$.To each primal cell K, we associate a center x_{K}. To each vertex x_{K^*} of the primal mesh, we associate a dual cell as shown in Fig. 2, by joining the surrounding centers. We use

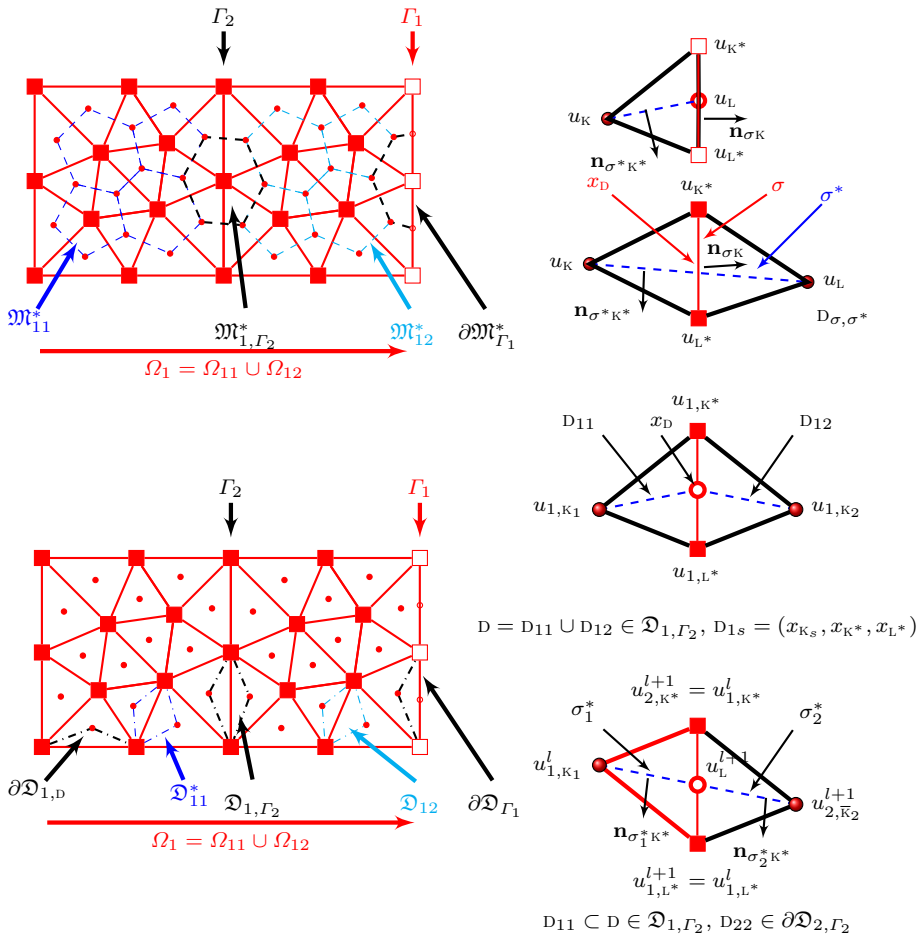

Fig. 2: Different dual cell sets (top left) and diamond cell sets (bottom left). Notations in the diamond cell (top right). Diamond cell in $\mathfrak{D}_{j,\Gamma_i}$ and $\partial\mathfrak{D}_{j,\Gamma_j}$ (bottom right).

analogous notation for the dual mesh, $\mathfrak{M}^*_j$, $\partial\mathfrak{M}^*_j$, $\partial\mathfrak{M}^*_{j,\mathrm{D}}$ and $\partial\mathfrak{M}^*_{\Gamma_j}$. The set of dual cells can be portioned into $\mathfrak{M}^*_j = \mathfrak{M}^*_{jj} \cup \mathfrak{M}^*_{ji} \cup \mathfrak{M}^*_{j,\Gamma_i}$ corresponding to cells included in Ω_{jj}, Ω_{ji} or crossing Γ_i as shown in Fig. 2. For both meshes, the intersection of two control volumes that is not empty or reduced to a vertex is called an edge. We define the diamond cells $\mathrm{D}_{\sigma,\sigma^*}$ as the quadrangles whose diagonals are a primal edge $\sigma = \mathrm{K}|\mathrm{L} = (x_{\mathrm{K}^*}, x_{\mathrm{L}^*})$ and a corresponding dual edge $\sigma^* = \mathrm{K}^*|\mathrm{L}^* = (x_{\mathrm{K}}, x_{\mathrm{L}})$. The set of diamond cells is called the diamond mesh, denoted by $\mathfrak{D}_j$.

For any C in $\mathcal{T}_j$, we denote by m_{C} its Lebesgue measure, by $\mathcal{E}_{\mathrm{C}}$ the set of its edges, and $\mathfrak{D}_{\mathrm{C}} := \{\mathrm{D}_{\sigma,\sigma^*} \in \mathfrak{D}_j,\ \sigma \in \mathcal{E}_{\mathrm{C}}\}$. For $\mathrm{D} = \mathrm{D}_{\sigma,\sigma^*}$ with vertices

$(x_{\mathrm{K}}, x_{\mathrm{K}^*}, x_{\mathrm{L}}, x_{\mathrm{L}^*})$, we denote by x_{D} the center of D, that is the intersection of the primal edge σ and the dual edge σ^*, by m_{D} its measure, by m_σ the length of σ, by m_{σ^*} the length of σ^*, by $m_{\sigma_{\mathrm{K}^*}}$ the length of $\partial\mathrm{K}^* \cap \Omega_j$, by $m_{\sigma_{\mathrm{L}}}$ the length of $\mathrm{D} \cap \partial\Omega_j$, and by $m_{\sigma_{\mathrm{K}}}$ the length of $[x_{\mathrm{K}}, x_{\mathrm{D}}]$. $\mathbf{n}_{\sigma\mathrm{K}}$ is the unit vector normal to σ oriented from x_{K} to x_{L}, and $\mathbf{n}_{\sigma^*\mathrm{K}^*}$ is the unit vector normal to σ^* oriented from x_{K^*} to x_{L^*}. We can split the set $\mathfrak{D}_j$ into $\mathfrak{D}_j^{int} \cup \mathfrak{D}_j^{ext}$ with $\mathfrak{D}_j^{int} = \mathfrak{D}_{jj} \cup \mathfrak{D}_{ji} \cup \mathfrak{D}_{j,\Gamma_i}$, $\mathfrak{D}_j^{ext} = \partial\mathfrak{D}_{j,\mathrm{D}} \cup \partial\mathfrak{D}_{\Gamma_j}$ corresponding to cells included in Ω_{jj}, Ω_{ji} or crossing Γ_i or boundary diamond cells as shown in Fig. 2.

The unknowns: the DDFV method associates to all primal control volumes $\mathrm{K} \in \mathfrak{M}_j \cup \partial\mathfrak{M}_j$ an unknown value $u_{j,\mathrm{K}}$, and to all dual control volumes $\mathrm{K}^* \in \mathfrak{M}_j^* \cup \partial\mathfrak{M}_j^*$ an unknown value u_{j,K^*}. We denote the approximate solution on the mesh $\mathcal{T}_j$ by $u_{\mathcal{T}_j} = ((u_{j,\mathrm{K}})_{\mathrm{K}\in(\mathfrak{M}_j\cup\partial\mathfrak{M}_j)}, (u_{j,\mathrm{K}^*})_{\mathrm{K}^*\in(\mathfrak{M}_j^*\cup\partial\mathfrak{M}_j^*)}) \in \mathbb{R}^{\mathcal{T}_j}$. When f is a continuous function, we define $f_{\mathcal{T}_j} = \mathbb{P}_c^{\mathcal{T}_j} f$ the evaluation of f on the mesh $\mathcal{T}_j$ defined for all control volumes $\mathrm{C} \in \mathcal{T}_j$ by $f_{\mathrm{C}} := f(x_{\mathrm{C}})$.

Operators. DDFV schemes can be described by two operators: a discrete gradient $\nabla^{\mathfrak{D}_j}$ and a discrete divergence $\mathrm{div}^{\mathcal{T}_j}$, which are dual to each other, see [1]. Let $\nabla^{\mathfrak{D}_j} : u_{\mathcal{T}_j} \in \mathbb{R}^{\mathcal{T}_j} \mapsto \left(\nabla^{\mathrm{D}} u_{\mathcal{T}_j}\right)_{\mathrm{D}\in\mathfrak{D}_j} \in (\mathbb{R}^2)^{\mathfrak{D}_j}$ and $\mathrm{div}^{\mathcal{T}_j} : \xi_{\mathfrak{D}_j} = (\xi_{j,\mathrm{D}})_{\mathrm{D}\in\mathfrak{D}_j} \in (\mathbb{R}^2)^{\mathfrak{D}_j} \mapsto \mathrm{div}^{\mathcal{T}_j}\xi_{\mathfrak{D}_j} \in \mathbb{R}^{\mathcal{T}_j}$ be defined as

$$\nabla^{\mathrm{D}} u_{\mathcal{T}_j} := \frac{1}{2m_{\mathrm{D}}}\left((u_{j,\mathrm{L}} - u_{j,\mathrm{K}})m_\sigma \mathbf{n}_{\sigma\mathrm{K}} + (u_{j,\mathrm{L}^*} - u_{j,\mathrm{K}^*})m_{\sigma^*}\mathbf{n}_{\sigma^*\mathrm{K}^*}\right), \quad \forall \mathrm{D} \in \mathfrak{D}_j,$$

$$\mathrm{div}^{\mathrm{K}}\xi_{\mathfrak{D}_j} := \frac{1}{m_{\mathrm{K}}} \sum_{\mathrm{D}\in\mathfrak{D}_{\mathrm{K}}} m_\sigma(\xi_{j,\mathrm{D}}, \mathbf{n}_{\sigma\mathrm{K}}), \ \forall \mathrm{K} \in \mathfrak{M}_j,$$

$$\mathrm{div}^{\mathrm{K}^*}\xi_{\mathfrak{D}_j} := \frac{1}{m_{\mathrm{K}^*}} \sum_{\mathrm{D}\in\mathfrak{D}_{\mathrm{K}^*}} m_{\sigma^*}(\xi_{j,\mathrm{D}}, \mathbf{n}_{\sigma^*\mathrm{K}^*}), \ \forall \mathrm{K}^* \in \mathfrak{M}_j^*.$$

DDFV scheme on Ω_j for Dirichlet boundary conditions on Γ_j. For $u_{\mathcal{T}_j} \in \mathbb{R}^{\mathcal{T}_j}$, $f_{\mathcal{T}_j} \in \mathbb{R}^{\mathcal{T}_j}$ and $h_{\mathcal{T}_j} \in \mathbb{R}^{\partial\mathfrak{M}_{\Gamma_j}\cup\partial\mathfrak{M}^*_{\Gamma_j}}$, the linear system denoted by $\mathcal{L}_{\Omega_j}^{\mathcal{T}_j}(u_{\mathcal{T}_j}, f_{\mathcal{T}_j}, h_{\mathcal{T}_j}) = 0$ refers to

$$-\mathrm{div}^{\mathrm{K}}\left(A_{\mathfrak{D}_j}\nabla^{\mathfrak{D}_j}u_{\mathcal{T}_j}\right) = f_{\mathrm{K}}, \quad \forall\ \mathrm{K} \in \mathfrak{M}_j, \tag{3}$$

$$-\mathrm{div}^{\mathrm{K}^*}\left(A_{\mathfrak{D}_j}\nabla^{\mathfrak{D}_j}u_{\mathcal{T}_j}\right) = f_{\mathrm{K}^*}, \quad \forall\ \mathrm{K}^* \in \mathfrak{M}_j^*, \tag{4}$$

$$u_{j,\mathrm{K}} = 0, \quad \forall\ \mathrm{K} \in \partial\mathfrak{M}_{j,\mathrm{D}}, \qquad u_{j,\mathrm{K}^*} = 0, \quad \forall\ \mathrm{K}^* \in \partial\mathfrak{M}^*_{j,\mathrm{D}}, \tag{5}$$

$$u_{j,\mathrm{L}} - \tfrac{m_{\mathrm{D}_{ii}}}{m_{\mathrm{D}}}u_{j,\mathrm{K}_j} = h_{j,\mathrm{L}}, \ \forall\ \mathrm{L} \in \partial\mathfrak{M}_{\Gamma_j}, \quad u_{j,\mathrm{K}^*} = h_{j,\mathrm{K}^*}, \ \forall\ \mathrm{K}^* \in \partial\mathfrak{M}^*_{\Gamma_j}, \tag{6}$$

where for all $\mathrm{L} \in \partial\mathfrak{M}_{\Gamma_j}$, we note that the edge associated to L belongs both to a diamond cell $\mathrm{D} \in \mathfrak{D}_{i,\Gamma_j}$ whose vertices are denoted by $x_{\mathrm{K}_1}, x_{\mathrm{K}_2}, x_{\mathrm{K}^*}, x_{\mathrm{L}^*}$ with $x_{\mathrm{K}_s} \in \Omega_{is}$ and to a boundary diamond cell $\mathrm{D}_{jj} \in \partial\mathfrak{D}_{i,\Gamma_j}$ whose vertices are denoted by $x_{\overline{\mathrm{K}}_j}, x_{\mathrm{K}^*}, x_{\mathrm{L}^*}$. We denote by the half-diamond D_{ii} the triangle whose vertices are $x_{\mathrm{K}_i}, x_{\mathrm{K}^*}, x_{\mathrm{L}^*}$ and by the half-diamond D_{jj} the triangle whose vertices are $x_{\overline{\mathrm{K}}_j}, x_{\mathrm{K}^*}, x_{\mathrm{L}^*}$ (See Fig. 2 bottom right). It is classical to see that this discrete formulation is well posed, see [1].

DDFV Schwarz method. The overlapping DDFV Schwarz method performs for an arbitrary initial guess $h^0_{\mathcal{T}_j} \in \mathbb{R}^{\partial\mathfrak{M}_{\Gamma_j}\cup\partial\mathfrak{M}^*_{\Gamma_j}}$, and $l = 1, 2, \dots$ the following steps (below either $(j,i) = (1,2)$ or $(j,i) = (2,1)$):

- Compute the solutions $u^{l+1}_{\mathcal{T}_j} \in \mathbb{R}^{\mathcal{T}_j}$ of $\mathcal{L}^{\mathcal{T}_j}_{\Omega_j}(u^{l+1}_{\mathcal{T}_j}, f_{\mathcal{T}_j}, h^l_{\mathcal{T}_j}) = 0$.
- Set $h^{l+1}_{j,\mathrm{K}^*} = u^{l+1}_{i,\mathrm{K}^*}$ for all $\mathrm{K}^* \in \partial\mathfrak{M}^*_{\Gamma_j}$, noting that $\mathrm{K}^* \in \mathfrak{M}^*_{i,\Gamma_j}$.
- Compute $h^{l+1}_{j,\mathrm{L}}$: there exists a unique value u^{l+1}_{L} such that

$$\left(A_{\mathrm{D}}\nabla^{\mathrm{D}_{ii}} u^{l+1}_{\mathcal{T}_i}, \mathbf{n}_{\sigma\mathrm{K}_i}\right) = \left(A_{\mathrm{D}}\nabla^{\mathrm{D}_{jj}} u^{l+2}_{\mathcal{T}_j}, \mathbf{n}_{\sigma\mathrm{K}_i}\right)$$

defined by

$$u^{l+1}_{\mathrm{L}} = \frac{m_{\mathrm{D}_i}}{m_{\mathrm{D}}} u^{l+2}_{j,\mathrm{K}_j} + \frac{m_{\mathrm{D}_j}}{m_{\mathrm{D}}} u^{l+1}_{i,\mathrm{K}_i} + \lambda_{\mathrm{D}}\left(u^{l+1}_{i,\mathrm{L}^*} - u^{l+1}_{i,\mathrm{K}^*}\right), \tag{7}$$

with $\lambda_{\mathrm{D}} = \frac{A_{\mathrm{D}}\mathbf{n}_{\sigma\mathrm{K}_j}\cdot\left(m_{\mathrm{D}_i} m_{\sigma^*_j}\mathbf{n}^j_{\sigma^*_{\mathrm{K}^*}} - m_{\mathrm{D}_j} m_{\sigma^*_i}\mathbf{n}^i_{\sigma^*_{\mathrm{K}^*}}\right)}{m_{\mathrm{D}} m_\sigma A_{\mathrm{D}}\mathbf{n}_{\sigma\mathrm{K}_1}.\mathbf{n}_{\sigma\mathrm{K}_1}}$ which equals zero in the case of classical DDFV meshes, *ie* $x_{\mathrm{D}} = (x_{\mathrm{K}_j}, x_{\mathrm{K}_i}) \cap (x_{\mathrm{K}^*}, x_{\mathrm{L}^*})$, see Fig 2. We then obtain

$$h^{l+1}_{j,\mathrm{L}} := \frac{m_{\mathrm{D}_j}}{m_{\mathrm{D}}} u^{l+1}_{i,\mathrm{K}_i} + \lambda_{\mathrm{D}}\left(u^{l+1}_{i,\mathrm{L}^*} - u^{l+1}_{i,\mathrm{K}^*}\right).$$

3 Convergence of overlapping DDFV Schwarz

The main difficulty to prove convergence of a Schwarz algorithm on non-matching grids is to identify its limit. In the conforming case, we will show that the limit is solution of a classical DDFV scheme on the entire domain, referred to as the monodomain solution. In the non-matching case, we will define two classical DDFV schemes on the entire domain, one associated to each subdomain, and then study numerically if convergence of the subdomain sequences occurs to their corresponding monodomain solution. To construct the monodomain solutions, consider $\bar{\mathcal{T}}_j$ the DDFV discretization of Ω associated to the primal mesh $\bar{\mathfrak{M}}_j = \mathfrak{M}_{jj} \cup \mathfrak{M}_{ji} \cup \mathfrak{M}_{ii}$. Note that in the conforming case, $\mathfrak{M}_{ji} = \mathfrak{M}_{ij}$, the extended meshes $\bar{\mathcal{T}}_1$ and $\bar{\mathcal{T}}_2$ coincide, and we denote them by $\bar{\mathcal{T}}$. The solution $\bar{u}^{\mathrm{DDFV}}_j$ of the classical monodomain DDFV scheme for homogeneous Dirichlet conditions is solution of the variational formulation (see e.g. [3])

$$a_j(\bar{u}^{\mathrm{DDFV}}_j, \bar{v}_{\bar{\mathcal{T}}_j}) := \sum_{\mathrm{D}\in\bar{\mathfrak{D}}_j} m_{\mathrm{D}} A_{\mathrm{D}}\nabla^{\mathrm{D}}\bar{u}_{\bar{\mathcal{T}}_j}\cdot\nabla^{\mathrm{D}}\bar{v}_{\bar{\mathcal{T}}_j} = \frac{1}{2}\sum_{\mathrm{K}\in\bar{\mathfrak{M}}_j} m_{\mathrm{K}} f_{\mathrm{K}}\bar{v}_{\mathrm{K}} + \frac{1}{2}\sum_{\mathrm{K}^*\in\bar{\mathfrak{M}}^*_j} m_{\mathrm{K}^*} f_{\mathrm{K}^*}\bar{v}_{\mathrm{K}^*}. \tag{8}$$

In each subdomain, we solve $\mathcal{L}^{\mathcal{T}_j}_{\Omega_j}(u^{l+1}_{\mathcal{T}_j}, f_{\mathcal{T}_j}, h^l_{\mathcal{T}_j}) = 0$, and extend the solution $u^{l+1}_{\mathcal{T}_j}$ to $\mathbb{R}^{\bar{\mathcal{T}}_j}$ using the previous iterate on the neighboring domain,

$$\bar{u}^{l+1}_{\overline{\mathcal{T}}_j} = \begin{cases} u^{l+1}_{\mathcal{T}_j} \text{ on } \mathbb{R}^{\mathfrak{M}_j \cup \mathfrak{M}^*_j}, \\ u^{l}_{\mathcal{T}_i} \text{ on } \mathbb{R}^{\mathfrak{M}^*_{i,\Gamma_j} \cup \mathfrak{M}_{ii} \cup \mathfrak{M}^*_{ii}}. \end{cases} \tag{9}$$

Introducing $V_j = \{\bar{v}_{\overline{\mathcal{T}}_j} \in \mathbb{R}^{\overline{\mathcal{T}}_j} \text{ such that } \bar{v}^{\mathfrak{M}_{ii} \cup \mathfrak{M}^*_{ii} \cup \mathfrak{M}^*_{i,\Gamma_j}} = 0\}$, by construction of the extension, we have $\bar{u}^{l+1}_{\overline{\mathcal{T}}_j} - \bar{u}^{l}_{\overline{\mathcal{T}}_i} \in V_j$ and for all $\bar{v}_{\overline{\mathcal{T}}_j} \in V_j$ we have $a_j(\bar{u}^{l+1}_{\overline{\mathcal{T}}_j} - \bar{u}^{\text{DDFV}}_j, \bar{v}_{\overline{\mathcal{T}}_j}) = 0$ since there exists $(\psi^{l+1}_{\mathrm{K}^*})_{\mathrm{K}^* \in \mathfrak{M}^*_{i,\Gamma_j}}$ and $(\psi^{l+1}_{\mathrm{K}_i})_{\mathrm{L} \in \partial\mathfrak{M}_{\Gamma_j}}$ such that

$$a_j(\bar{u}^{l+1}_{\overline{\mathcal{T}}_j}, \bar{v}_{\overline{\mathcal{T}}_j}) = \frac{1}{2} \sum_{\mathrm{K} \in \bar{\mathfrak{M}}_j} m_{\mathrm{K}} f_{\mathrm{K}} \bar{v}_{\mathrm{K}} + \frac{1}{2} \sum_{\mathrm{K}^* \in \bar{\mathfrak{M}}^*_j} m_{\mathrm{K}^*} f_{\mathrm{K}^*} \bar{v}_{\mathrm{K}^*} + \sum_{\mathrm{K}^* \in \mathfrak{M}^*_{i,\Gamma_j}} \bar{v}_{\mathrm{K}^*} \psi^{l+1}_{\mathrm{K}^*} + \sum_{\mathrm{L} \in \partial\mathfrak{M}_{\Gamma_j}} \bar{v}_{\mathrm{K}_i} \psi^{l+1}_{\mathrm{K}_i}.$$

Theorem 1 *If the meshes are conforming, $\mathcal{M}_{ij} = \mathcal{M}_{ji}$, then the DDFV Schwarz algorithm converges in the discrete DDFV H^1 semi-norm*

$$\|\bar{u}_{\overline{\mathcal{T}}_j}\|_{H^1} := \Big(\sum_{\mathrm{D} \in \bar{\mathfrak{D}}_j} m_{\mathrm{D}} \|\nabla^{\mathrm{D}} \bar{u}_{\overline{\mathcal{T}}_j}\|^2 \Big)^{\frac{1}{2}}. \tag{10}$$

Proof If $\mathcal{M}_{ij} = \mathcal{M}_{ji}$, then $a_j = a_i := a$, and we obtain that $a(\bar{u}^{l+1}_{\overline{\mathcal{T}}_j} - \bar{u}^{l}_{\overline{\mathcal{T}}_i}, \bar{v}_{\overline{\mathcal{T}}_j}) = 0$ for all $\bar{v}_{\overline{\mathcal{T}}_j} \in V_j$ and thus $\bar{u}^{l+1}_{\overline{\mathcal{T}}_j} - \bar{u}^{l}_{\overline{\mathcal{T}}_i}$ is the orthogonal projection of $\bar{u}^{\text{DDFV}}_j - \bar{u}^{l}_{\overline{\mathcal{T}}_i}$ onto V_j with respect to the scalar product induced by a. Now because $\mathbb{R}^{\overline{\mathcal{T}}} = V_1 + V_2$, we can apply [7, Lemma 2.12 and Theorem 2.15] (see also [2, Fig. 2.4]) to conclude that the proposed overlapping DDFV Schwarz method converges geometrically to the monodomain DDFV solution in the norm induced by a or equivalently for the discrete DDFV H^1 semi-norm (10). □

If the meshes are non-conforming, $\mathcal{M}_{ij} \neq \mathcal{M}_{ji}$, we have two monodomain solutions, one from extending each subdomain mesh to the overall domain, and neither convergence nor the limit of the DDFV Schwarz algorithm is known. We thus study now numerically its convergence, for both the conforming and non-conforming cases. We use a strong anisotropy $A = \left(\begin{smallmatrix} 1.5 & 0.5 \\ 0.5 & 15 \end{smallmatrix}\right)$ and a manufactured solution $u_e(x, y) = \sin(\pi x)\sin(\pi y)\sin(\pi(x + y))$ putting the corresponding source term f and non homogeneous boundary conditions on $(-0.75, 0.75) \times (0, 1)$. The overlap is $(-0.25, 0.25) \times (0, 1)$. The meshes are built using refinements of the meshes shown in Fig. 1. For both families, $\mathfrak{M}_{11}$ is the triangle mesh and $\mathfrak{M}_{22}$ is the square mesh, and in the conforming case $\mathfrak{M}_{12}$ and $\mathfrak{M}_{21}$ are both the square mesh, while in the nonconforming case $\mathfrak{M}_{12}$ is the triangle mesh and $\mathfrak{M}_{21}$ is the square mesh. Note that the dual meshes exhibit a large variety of polygonal cells. Tables 1 and 2 show a detailed error analysis of the results we obtain, stopping the algorithm as soon as $\|u^l - u^{l-1}\|_{L^2} \leq 1e-13$ with

#cells	cellsize	$\|u^{l+1}-u^l\|_{H^1}$	$\|u^l-\bar{u}^{\mathrm{DDFV}}\|_{H^1}$	$\|u^l-\mathbb{P}_c^\tau u_e\|_{H^1}$	order	$\|u^l-\mathbb{P}_c^\tau u_e\|_{L^2}$	order
140	3.5E-01	2.080E-15	4.062E-16	1.355E-01	—	1.086E-01	—
458	1.8E-01	1.360E-15	1.022E-15	5.945E-02	1.19	2.897E-02	1.91
1634	8.8E-02	3.662E-14	1.911E-15	3.104E-02	0.94	7.998E-03	1.86
6146	4.4E-02	2.537E-14	8.703E-15	1.563E-02	0.99	2.071E-03	1.95
23810	2.2E-02	2.694E-14	1.945E-14	7.737E-03	1.01	5.228E-04	1.99
93698	1.1E-02	3.561E-14	3.139E-14	3.832E-03	1.01	1.311E-04	2.00

Table 1: Conforming overlap: convergence of the Schwarz algorithm $\|u^{l+1}-u^l\|_{H^1} \to 0$ and convergence to the monodomain solution $\bar{u}^{\mathrm{DDFV}}$ for all mesh sizes; convergence under mesh refinement of the limit of the Schwarz algorithm to the exact solution of order 1 in H^1 and order 2 in L^2.

#cells	cellsize	$\|u^{l+1}-u^l\|_{H^1}$	$\|u^l-\bar{u}^{\mathrm{DDFV}}\|_{H^1}$	order	$\|u^l-\mathbb{P}_c^\tau u_e\|_{H^1}$	order	$\|u^l-\mathbb{P}_c^\tau u_e\|_{L^2}$	order
166	3.5E-01	3.497E-15	3.875E-02	—	1.469E-01	—	1.207E-01	—
562	1.8E-01	1.079E-14	1.833E-02	1.08	5.987E-02	1.29	2.930E-02	2.04
2050	8.8E-02	8.451E-14	6.271E-03	1.55	3.233E-02	0.89	8.178E-03	1.84
7810	4.4E-02	6.264E-14	1.830E-03	1.78	1.677E-02	0.95	2.153E-03	1.93
30466	2.2E-02	4.514E-14	5.152E-04	1.83	8.448E-03	0.99	5.498E-04	1.97

Table 2: Non conforming overlap: as for Table 1, but only convergence under mesh refinement to the monodomain solution $\bar{u}^{\mathrm{DDFV}}$.

#cells	cellsize	$\|u^l-u^{l-1}\|_{H^1}$	$\|u^l-\bar{u}^{\mathrm{DDFV}}\|_{H^1}$	$\|u^l-\mathbb{P}_c^\tau u_e\|_{H^1}$	order	$\|u^l-\mathbb{P}_c^\tau u_e\|_{L^2}$	order
166	3.54E-01	1.183E-13	2.412E-14	7.521E-03	—	1.366E-03	—
562	1.77E-01	7.843E-14	1.569E-14	3.769E-03	1.00	3.315E-04	2.04
2050	8.84E-02	7.024E-14	1.448E-14	1.886E-03	1.00	8.154E-05	2.02
7810	4.42E-02	7.071E-14	2.165E-14	9.434E-04	1.00	2.022E-05	2.01
30466	2.21E-02	7.668E-14	1.193E-13	4.718E-04	1.00	5.034E-06	2.00

Table 3: Case $u_e(x,y) = xy$ and $A = Id$ and convergence of $\|u^l-\bar{u}^{\mathrm{DDFV}}\|_{H^1}$ as in the conforming case of Table 1, even thought the mesh is non-conforming!

$$\|\bar{u}_{\bar{\mathcal{T}}_j}\|_{L^2} := \sqrt{\sum_{\mathrm{K}\in\mathfrak{M}_j} m_{\mathrm{K}}\bar{u}_{\mathrm{K}}^2} + \sqrt{\sum_{\mathrm{K}^*\in\mathfrak{M}_j{}^*\cup\partial\mathfrak{M}_j^*} m_{\mathrm{K}^*}\bar{u}_{\mathrm{K}^*}^2}.$$

In the third column we see that the algorithm converges in all cases in the relative discrete H^1-norm (10) defined for $u_\mathcal{T}-v_\mathcal{T}$ by $\|u_\mathcal{T}-v_\mathcal{T}\| := \frac{\|u_\mathcal{T}-v_\mathcal{T}\|_{H^1}}{\|v_\mathcal{T}\|_{H^1}}$. The fourth column in Table 1 shows convergence to the monodomain solution for conforming meshes as proved in Theorem 1, but only convergence under mesh refinement in the non-conforming case in Table 2. The remaining columns show that the limits of the Schwarz algorithm converge always under mesh refinement to the evaluation $\mathbb{P}_c^\tau u_e$ of the exact solution u_e on the meshes, of order 1 in H^1 and order 2 in L^2, for an illustration of the converged solution, see Fig. 3. We observe however also several cases where $\bar{u}^{\mathrm{DDFV}}$ corresponds to the limit of u^l even in the nonconforming case, e.g. for $u_e = 0$ or $u_e(x,y) = xy$ with $A = Id$ as shown in Table 3. The complete understanding

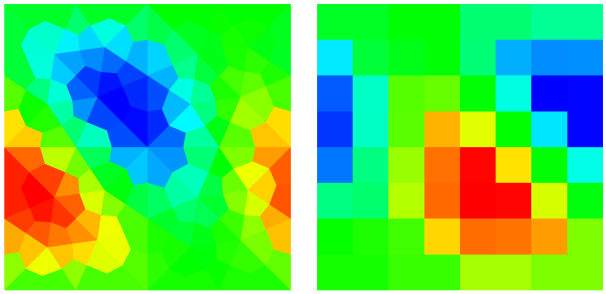

Fig. 3: u_1^l (left) and u_2^l (right) after $l = 21$ iterations on the primal non-conforming meshes with refinement 2, corresponding to 562 unknowns.

of convergence to the mono-domain solution in the non-conforming case thus requires a deeper study of the limiting equations of the overlapping Schwarz process when discretized by nonconforming DDFV.

References

1. Boris Andreianov, Franck Boyer, and Florence Hubert. Discrete duality finite volume schemes for Leray-Lions type problems on general 2D meshes. *Numerical Methods for PDE*, 23(1):145–195, 2007.
2. Gabriele Ciaramella and Martin J. Gander. Analysis of the parallel Schwarz method for growing chains of fixed-sized subdomains: Part III. *ETNA*, 49:201–243, 2018.
3. K. Domelevo and P. Omnes. A finite volume method for the Laplace equation on almost arbitrary two-dimensional grids. *M2AN Math. Model. Numer. Anal.*, 39(6):1203–1249, 2005.
4. Martin J Gander, Laurence Halpern, Florence Hubert, and Stella Krell. Optimized overlapping DDFV Schwarz algorithms. In Klöfkorn R., Keilegavlen E., Radu F., and Fuhrmann J., editors, *Finite Volumes for Complex Applications IX - Methods, Theoretical Aspects, Examples. FVCA 2020.*, volume 323 of *Proceedings in Mathematics & Statistics.*, pages 365–373. Springer, 2020.
5. Martin J. Gander, Laurence Halpern, Florence Hubert, and Stella Krell. Optimized Schwarz Methods for Anisotropic Diffusion with Discrete Duality Finite Volume Discretizations. *Moroccan Journal of Pure and Applied Analysis*, 7(2):182–213, July 2021.
6. F. Hermeline. Approximation of diffusion operators with discontinuous tensor coefficients on distorted meshes. *Comput. Methods Appl. Mech. Engrg.*, 192(16-18):1939–1959, 2003.
7. Pierre-Louis Lions. On the Schwarz alternating method. I. In *First international symposium on domain decomposition methods for partial differential equations*, volume 1, page 42. Paris, France, 1988.
8. B. Smith, P. Bjørstad, and W. Gropp. *Domain Decomposition: Parallel Multilevel Methods for Elliptic Partial Differential Equations*. Cambridge University Press, 1996.